

# Nucleon-Nucleon Scattering in a Harmonic Potential

Thomas Luu,<sup>1,\*</sup> Martin Savage,<sup>2,†</sup> Achim Schwenk,<sup>3,4,5,‡</sup> and James P. Vary<sup>6,§</sup>

<sup>1</sup>*N Section, Lawrence Livermore National Laboratory, Livermore, CA 94551, USA*

<sup>2</sup>*Department of Physics, University of Washington, Seattle, WA 98195-1560, USA*

<sup>3</sup>*ExtreMe Matter Institute EMMI, GSI Helmholtzzentrum für  
Schwerionenforschung GmbH, 64291 Darmstadt, Germany*

<sup>4</sup>*Institut für Kernphysik, Technische Universität Darmstadt, 64289 Darmstadt, Germany*

<sup>5</sup>*TRIUMF, 4004 Wesbrook Mall, Vancouver BC, V6T 2A3, Canada*

<sup>6</sup>*Department of Physics and Astronomy,  
Iowa State University, Ames, IA 50011, USA*

(Dated: May 24, 2022)

## Abstract

The discrete energy-eigenvalues of two nucleons interacting with a finite-range nuclear force and confined to a harmonic potential are used to numerically reconstruct the free-space scattering phase shifts. The extracted phase shifts are compared to those obtained from the exact continuum scattering solution and agree within the uncertainties of the calculations. Our results suggest that it might be possible to determine the amplitudes for the scattering of complex systems, such as  $nd$ ,  $nt$  or  $n\alpha$ , from the energy-eigenvalues confined to finite volumes using *ab-initio* bound-state techniques.

---

\*tluu@llnl.gov

†mjs5@u.washington.edu

‡schwenk@physik.tu-darmstadt.de

§jvary@iastate.edu

## I. INTRODUCTION

Quantum scattering of strongly interacting few-nucleon systems is complicated and requires careful treatment of asymptotics, antisymmetrization effects as well as the dynamics generated by nuclear forces. Full treatments of antisymmetrization with correlations have become routine in bound-state and quasi-bound-state solutions of light nuclei using *ab-initio* techniques based on nucleon-nucleon ( $NN$ ) and three-nucleon interactions ( $3N$ ). Techniques, such as the No Core Shell Model (NCSM) (see, e.g., Ref. [1, 2]), Green's Function Monte Carlo (GFMC) (see, e.g., Ref. [3, 4]), and the Coupled Cluster (CC) approach (see, e.g., Ref. [5, 6]), are used to calculate ground and excited states of light nuclei. The precision of these calculations has reached a point where further progress is now limited by the fidelity of the input interactions.

In reaction calculations of scattering properties of light nuclei, progress has been less pronounced, though nonetheless significant. R-matrix analysis (see, e.g., Ref. [7, 8]) has been historically the empirical workhorse, providing impressive fits to a range of experimental data. More microscopic approaches to the scattering of light nuclei are based on the Resonating Group Method (RGM) [9–11]. A promising avenue for *ab-initio* calculations of scattering of light ions comes from the coupling of the RGM reaction method with the NCSM bound-state technique [12]. For this method, the large computational resources required to achieve convergence provide the limiting constraint on reliably calculating scattering parameters for processes with  $A > 5$ . It would be significant if existing bound-state techniques, and their accompanying precision, could be further exploited to reliably determine scattering amplitudes for multi-nucleon systems.

During the last twenty years the general technique of effective field theory (EFT) has been developed and applied to multi-nucleon systems. Effective Field Theory provides a description of observables, consistent with the approximate chiral symmetries of quantum chromodynamics (QCD), in terms of a small number of expansion parameters within a plane-wave basis. These expansion parameters are used to relate the experimentally determined scattering parameters and bound-state properties of few-nucleon systems to the coefficients of operators at a given order in the EFT expansion. In principle, this allows for systematically improvable calculations of multi-nucleon observables. Applying the EFT framework within an oscillator basis has also been investigated [13–15]. More recently, it has been suggested that the EFT framework might be fruitfully applied to multi-fermion systems confined in a harmonic potential [16–18], and might be usefully married with the NCSM calculational scheme. In Ref. [19] it was suggested that the scattering properties of certain complex nuclear systems could be calculated from the spectrum of the same systems confined to a harmonic potential. This was demonstrated for two confined particles at the unitary limit in Ref. [20]. A lattice formulation of EFT coupled with an external harmonic potential is currently being developed [21].

In this work we investigate the simple two-nucleon system confined in a harmonic potential of the form  $V_{HO} = \frac{1}{2}M_N\omega^2r^2$ , and interacting via nuclear forces in uncoupled partial waves. Since two-body techniques are well established for both scattering and bound states, this system is ideal for determining the extent to which continuum scattering amplitudes can be recovered from bound-state information. An analytic expression that relates the eigenvalues of two interacting particles moving in a harmonic potential to the scattering phase shift at those energies, analogous to “Lüscher's method” [22–24] that is used in Lattice QCD, allows for the scattering phase shift to be determined in the limit that the oscillator

length is large compared to the range of nuclear forces. As the latter is characterized by the Compton wavelength of the pion, with increasing confinement this leads to modifications to nuclear forces due to the harmonic potential that must be systematically removed in order to accurately predict the scattering amplitude. This is achieved by calculating the energy-eigenvalues over a range of harmonic frequencies,  $\omega$ , determining the scattering amplitude over this range of  $\omega$ , and then extrapolating to the  $\omega = 0$  limit. We verify the extracted phase shifts by comparing them to the results of an independent scattering calculation. The two methods are found to yield the same phase shifts within the uncertainties of the calculations.

## II. PHASE SHIFTS FROM THE ZERO-RANGE RELATION

It is well-established that the energy-eigenvalues of an interacting system of particles confined to a finite volume can be used to determine the scattering phase shift (at the energy-eigenvalues) when the size of the confining region is much larger than the range of the interactions between the particles. For instance, relating the scattering phase shift to the energy-eigenvalues of two-nucleons confined to a spherical region by solving the Schrödinger equation with a Dirichlet boundary condition is a problem that appears in standard texts on nuclear physics, see, e.g., Ref. [25]. This method has been successfully employed in the latticization of low-energy EFT's to predict (to a given level of precision) the ground state energies of light nuclei and their volume dependence [26].

Volume dependence is also used to determine meson-meson, meson-baryon and baryon-baryon elastic scattering phase shifts from the energy-eigenvalues of these systems calculated with Lattice QCD <sup>1</sup> (for a recent review, see Ref. [28]). Lattice QCD calculations are generally performed in spatial volumes with cubic symmetry and with periodic boundary-conditions (BC's) imposed upon the fields at the edges. This reduces the number of momentum modes, and hence reduces the kinetic-energy contributions to the calculated processes. The non-relativistic relation between the energy-eigenvalues and the scattering amplitude (the “Lüscher relation”) has been shown to be valid even in quantum field theory [23, 24]. Given the energy-splitting,  $\Delta E_n$ , between the two-hadron state and the hadron masses,  $m$ , the real part of the inverse scattering amplitude below inelastic thresholds is

$$p_n \cot \delta(p_n) = \frac{1}{\pi L} \mathbf{S} \left( \left( \frac{p_n L}{2\pi} \right)^2 \right) , \quad \mathbf{S}(x) \equiv \sum_{|\mathbf{j}| < \Lambda} \frac{1}{|\mathbf{j}|^2 - x} - 4\pi\Lambda , \quad (1)$$

where  $\Delta E_n = 2\sqrt{p_n^2 + m^2} - 2m$ ,  $\delta(p_n)$  is the energy-dependent phase-shift, and the limit  $\Lambda \rightarrow \infty$  is implicit. The  $\mathbf{S}$ -function is the Green function,  $G_{HH}(\mathbf{0}, \mathbf{0})$ , for two-hadron plane-wave eigenstates (and straightforwardly generalizes to hadrons with different masses). The Lüscher relation between the scattering amplitude and the energy-eigenvalues in the finite lattice volume, given by Eq. (1), is valid when the spatial extent of the lattice is large compared to the range of the interaction,  $R$ . Corrections to the relation are found to behave as  $\sim e^{-L/R}$ , see, e.g., Ref. [29]. If, in the continuum (infinite-volume) limit, a system contains a shallow bound state, as is the case in the NN  ${}^3S_1$ - ${}^3D_1$  coupled channel, the periodic BC

---

<sup>1</sup> The Maiani-Testa theorem [27] precludes the extraction of scattering matrix elements from Euclidean-space Green functions in the infinite-volume limit except at kinematic thresholds.

in a finite volume increases the binding energy of the state. The finite-volume corrections scale as  $e^{-\gamma_0 L}$  [30], where  $\gamma_0$  is the binding momentum in the continuum. In contrast, the continuum scattering states have power-law dependences upon the lattice extent for  $L \gg R$ , with energies that behave as  $\sim 1/L^3$  for the ground state and  $\sim 1/L^2$  for the higher-energy states.

The systems that we considered in this work are comprised of two nucleons in a harmonic potential (with oscillator frequency  $\omega$ ) interacting through NN forces. We will consider the JISP16 potential [31–33], which reproduces the low-energy NN scattering data with a  $\chi^2/\text{dof} \sim 1.0$ , but our results are general and the technique can be applied to other NN interactions. The EFT-method that was used to (re-)derive the Lüscher relation in Eq. (1) in non-relativistic quantum mechanics [30], can be used to (re-)derive the relation between  $p^{2l+1} \cot \delta_l(p)$  in an uncoupled partial wave with angular momentum  $l$  and the energy-eigenvalues of two nucleons in a harmonic potential [35–37],

$$p^{2l+1} \cot \delta_l(p) = (-1)^{l+1} (2m\omega)^{l+1/2} \frac{\Gamma\left(\frac{2l+3}{4} - \frac{\epsilon}{2}\right)}{\Gamma\left(\frac{1-2l}{4} - \frac{\epsilon}{2}\right)}, \quad (2)$$

where  $\epsilon = E/\omega$  and  $E = p^2/m$  is the fully interacting energy in the center of mass frame. While the EFT derivation using the pionless-EFT is valid only up to momenta associated with the cut in the t-channel from the exchange of one pion, the relation is valid up to the inelastic threshold. Equation (2), like the Lüscher formula, is valid in the limit of zero-range interactions. The harmonic potential, being non-zero everywhere, except at the origin, modifies the interaction between the two nucleons, and the  $NN$  phase shift at the outer range of the nuclear potential differs from that in free space. This is a finite-range effect, and unlike the situation encountered in Lattice QCD calculations, it is not expected to be exponentially suppressed (in  $\omega$ ). Equation (2), in conjunction with the leading order (LO) term in the effective range expansion (ERE) of  $p \cot \delta$ , the scattering length  $a$ , has been used to determine the spectrum of dilute cold atoms in traps with essentially zero-range interactions, particularly in the vicinity of Feshbach resonances [35–38]. On the other hand, since Eq. (2) relates the energy-dependent phase shift to the energy-eigenvalues  $E$  of the confined system, knowledge of the spectrum of the two-particle system allows the extraction of the continuum scattering amplitude up to finite-range corrections.

### A. Loosely Bound States in Weak Harmonic Potentials

For attractive  $S$ -wave interactions with positive scattering length,  $a_0 > 0$ , a bound state exists and the binding energy  $B_0$  can be written in terms of the binding momentum,  $\gamma_0$ ,

$$B_0 \equiv \frac{\gamma_0^2}{m},$$

where  $\gamma \sim 1/a$  for scattering lengths large compared to the range of the interaction. Refining the estimate of the binding energy gives  $\gamma$  as the solution to

$$\frac{1}{a_0} + \frac{1}{2} r_0 \gamma_0^2 - \gamma_0 = 0, \quad (3)$$

where  $r_0$  is the effective range of the interaction, and the ERE of  $p \cot \delta = -\frac{1}{a_0} + \frac{1}{2} r_0 p^2 + \dots$  has been truncated at second order, which, in the case of  $S$ -wave interactions between

nucleons, is sufficient for most purposes. The presence of the harmonic potential, and in particular its non-zero value throughout the volume of the bound-state, gives rise to a power-law modification to the binding energy [35], even in the limit of zero-range interactions. The location of the state corresponding to the free-space bound-state can be found directly from Eq. (2) in the zero-range limit, and for small  $\omega$  the shift in the energy of the bound-state is perturbative in  $\omega^2$ ,

$$B_\omega = B_0 - \frac{1}{8(1-\gamma_0 r_0)} \frac{\omega^2}{B_0} + O(\omega^4) = B_0 - C_{ZR} \omega^2 + O(\omega^4) \quad , \quad (4)$$

where we define  $C_{ZR} = [8B_0(1-\gamma_0 r_0)]^{-1}$  for later reference. Equation (4) indicates that, given the bound-state energy  $B_\omega$  calculated at different values of  $\omega$ , the continuum binding energy  $B_0$  could be determined by an extrapolation in  $\omega^2$  to  $\omega = 0$ . This same extrapolation can also be done in the presence of finite-range corrections since, as we show later, these corrections occur at order  $\omega^2$  for small  $\omega$ . In the  ${}^3S_1$ - ${}^3D_1$  coupled-channels that contain the deuteron with binding-energy  $B_0 = 2.224575$  MeV ( $\gamma_0 \sim 45.7$  MeV) and with an S-wave effective range of  $r_0 \sim 1.74$  fm, the coefficient is  $C_{ZR} = 0.0944$  MeV $^{-1}$ .

The LO shift in the bound-state energy given in eq. (4) can be recovered from the bound-state wavefunction based on ERE,

$$\psi^{(ER)}(r) = \psi_{\text{short}}(r) + \sqrt{\frac{\gamma_0}{2\pi}} \frac{1}{\sqrt{1-\gamma_0 r_0}} \frac{e^{-\gamma_0 r}}{r} \quad , \quad (5)$$

where  $\psi_{\text{short}}(r)$  is the short-distance component of the wavefunction that has support over a radius  $r \ll \gamma_0^{-1}$ . The factor of  $1/\sqrt{1-\gamma_0 r_0}$  in eq. (5) is determined by the residue of the pole in the scattering amplitude. At LO in perturbation theory, the contribution to the energy of this state from the harmonic potential is

$$\Delta E_0 = \langle \psi^{(ER)} | \frac{1}{2} m \omega^2 r^2 | \psi^{(ER)} \rangle = \frac{1}{8(1-\gamma_0 r_0)} \frac{\omega^2}{B_0} + \text{short-distance} \quad , \quad (6)$$

in agreement with the result in eq. (4).

## B. Scattering States in Weak Harmonic Potentials

It is useful to construct perturbative expansions for the energy-eigenvalues in the zero-range limit. As we show later in sect. IV A, these relations can be used to readily extract effective range parameters given the low energy spectrum of the system. Using the zero-range relation given in eq. (2) it is straightforward to determine the location of the energy-eigenstates in the limit that  $\sqrt{m\omega}/(p \cot \delta) \ll 1$ , and also in the unitary-limit where  $\sqrt{m\omega}/(p \cot \delta) \gg 1$ . In the  $\sqrt{m\omega}/(p \cot \delta) \ll 1$  limit, the  $q^{\text{th}}$  energy-level with orbital angular momentum  $l$  is

located at

$$\begin{aligned} \frac{E_q^{(l)}}{\omega} = & \left( \frac{3}{2} + l + 2q \right) \\ & + 2 \left[ \left( \frac{\sqrt{2}}{b} \right)^{2l+1} \frac{(-)^{l+q}}{\Gamma[1+q] \Gamma[-\frac{1}{2} - l - q] p^{2l+1} \cot \delta_l(E_0)} \right. \\ & \left. + \left( \frac{\sqrt{2}}{b} \right)^{4l+2} \frac{H(-\frac{3}{2} - l - q) - H(q)}{[\Gamma[1+q] \Gamma[-\frac{1}{2} - l - q] p^{2l+1} \cot \delta_l(E_0)]^2} + \dots \right], \quad (7) \end{aligned}$$

where  $E_0 = \frac{1}{mb^2} (\frac{3}{2} + l + 2q)$  with  $b = 1/\sqrt{m\omega}$ , and the  $H(x)$  are harmonic numbers<sup>2</sup>. When applied to the lowest-lying S-wave state, one finds that, for small- $\omega$ ,

$$\frac{E_0^{(0)}}{\omega} = \frac{3}{2} - \frac{1}{bp \cot \delta_0} \left( \sqrt{\frac{2}{\pi}} - \frac{2(1 - \log 2)}{\pi bp \cot \delta_0} - \frac{\pi^2 - 24 + 36(2 - \log 2) \log 2}{6\sqrt{2}\pi^{3/2} (bp \cot \delta_0)^2} + \dots \right), \quad (8)$$

where  $p \cot \delta_0$  is evaluated at  $p^2/m = 3\omega/2$ <sup>3</sup>. The first excited S-wave state is located at

$$\begin{aligned} \frac{E_1^{(0)}}{\omega} = & \frac{7}{2} \\ & - \frac{1}{bp \cot \delta_0} \left( \frac{3}{\sqrt{2\pi}} + \frac{3(6 \log 2 - 5)}{4\pi bp \cot \delta_0} - \frac{3(3\pi^2 - 4(11 + 9 \log 2(3 \log 2 - 5)))}{6\sqrt{2}\pi^{3/2} (bp \cot \delta_0)^2} + \dots \right), \quad (9) \end{aligned}$$

where  $p \cot \delta_0$  is evaluated at  $p^2/m = 7\omega/2$ . The finite range corrections to these expressions can be introduced by replacing  $p \cot \delta_0 \rightarrow p \cot \delta_0 + A\omega^2 + \dots$  for small  $\omega$ , where the finite-range corrections depend upon the interaction, and cannot be determined from scattering parameters alone. It makes little sense to continue the expansion in  $\sqrt{m\omega}/(p \cot \delta)$  to higher orders due to the appearance of the range corrections.

The same expansion can be applied to the P-waves, for which the expansion is in terms of  $(m\omega)^{3/2}/(p^3 \cot \delta_1) \ll 1$ . The lowest-lying continuum state is located at

$$\frac{E_0^{(1)}}{\omega} = \frac{5}{2} - \frac{3\sqrt{\frac{2}{\pi}}}{b^3 p^3 \cot \delta_1} - \frac{6(3 \log 2 - 4)}{\pi (b^3 p^3 \cot \delta_1)^2} + \dots, \quad (10)$$

with  $p^3 \cot \delta_1$  evaluated at  $p^2/m = 5\omega/2$ , the first excited state is located at

$$\frac{E_1^{(1)}}{\omega} = \frac{9}{2} - \frac{\frac{15}{\sqrt{2\pi}}}{b^3 p^3 \cot \delta_1} - \frac{15(30 \log 2 - 31)}{4\pi (b^3 p^3 \cot \delta_1)^2} + \dots, \quad (11)$$

<sup>2</sup> Our definition of the oscillator parameter differs from that of Ref. [20] by a factor of  $\sqrt{2}$ .

<sup>3</sup> To recover the results of Ref. [20],  $p \cot \delta_0$  is replaced by the ERE evaluated at  $p^2/m = 3\omega/2$ ,

$$p \cot \delta_0 = -\frac{1}{a_0} + \frac{3}{2} \frac{r_0}{2} m\omega + \dots,$$

and eq. (8) is then re-arranged in powers of  $b^{-1}$ .

with  $p^3 \cot \delta_1$  evaluated at  $p^2/m = 9\omega/2$ , and the second excited state is located at

$$\frac{E_2^{(1)}}{\omega} = \frac{13}{2} - \frac{\frac{105}{4\sqrt{2}\pi}}{b^3 p^3 \cot \delta_1} - \frac{105(410 \log 2 - 389)}{128\pi (b^3 p^3 \cot \delta_1)^2} + \dots, \quad (12)$$

with  $p^3 \cot \delta_1$  evaluated at  $p^2/m = 13\omega/2$ .

The limit of large scattering length,  $a/b \gg 1$ , and small range,  $r/b \ll 1$ , the unitary limit, can also be considered. An expansion in powers of  $p \cot \delta_0 / (m\omega)^{1/2}$  can be performed, and the lowest-lying S-wave state is located (by expanding about the poles in the denominator of eq. (2) ) at

$$\frac{E_0^{(0)}}{\omega} = \frac{1}{2} + \sqrt{\frac{2}{\pi}} \frac{p \cot \delta_0}{\sqrt{m\omega}} + \dots, \quad (13)$$

where  $p \cot \delta_0$  is evaluated at  $p^2/m = \omega/2$ . This generalizes the results of Ref. [35].

### III. A TOY MODEL

For a harmonic potential with an arbitrary value of  $\omega$  one must rely on eq. (2) to extract continuum phase shifts and scattering parameters from the location of the energy-eigenvalues, while keeping in mind that finite-range effects are present and will move the calculated phase shift away from its true value. To test the utility of eq. (2) in the presence of a finite-range interaction and to develop a “feel” for the size of the finite-range corrections, we use the toy example of two particles interacting via a spherical well. To make this system as ‘nuclear-like’ as possible, the depth and width of the well are tuned to reproduce gross features of the deuteron system. In particular, with a well depth  $V_0 = 48$  MeV and radius  $R_0 = 1.7$  fm, the single bound state has a binding energy  $B_0 = 2.22$  MeV. The scattering phase shift for this potential is known to be

$$\delta_0 = \tan^{-1} \left[ \sqrt{\frac{E_{\text{lab}}}{E_{\text{lab}} + 2V_0}} \tan \left( \sqrt{R_0 \mu (E_{\text{lab}} + 2V_0)} \right) \right] - \sqrt{E_{\text{lab}} R_0^2 V_0 \mu}, \quad (14)$$

where  $\mu$  is the reduced mass.

This system is placed within a harmonic potential and the resulting two-body spectrum at various oscillator frequencies is determined numerically. For each oscillator frequency, the spectrum is used to extract the scattering phase shift by virtue of eq. (2). Because the spectrum is discretized, the extracted phase shifts occur at discrete points. By varying the oscillator frequency, the energies at which the phase shift is determined vary thereby allowing for the energy-dependence of the phase shift to be mapped out.

For modest-sized oscillator frequencies ( $\omega < 4$  MeV) the extracted phase shifts agree well with the exact result given in eq. (14) (within 0.1%), as shown in Fig. 1, as the effects of the harmonic potential are negligible within the range of the spherical well. The situation changes, however, for large oscillator frequencies, also shown in Fig. 1. In this case the exact phase shifts and extracted phase shifts have appreciable differences due to the finite range of the spherical well. Not surprisingly, the confining nature of these potentials distorts the interaction of the two particles within the spherical well, which is demonstrated in Fig. 2.

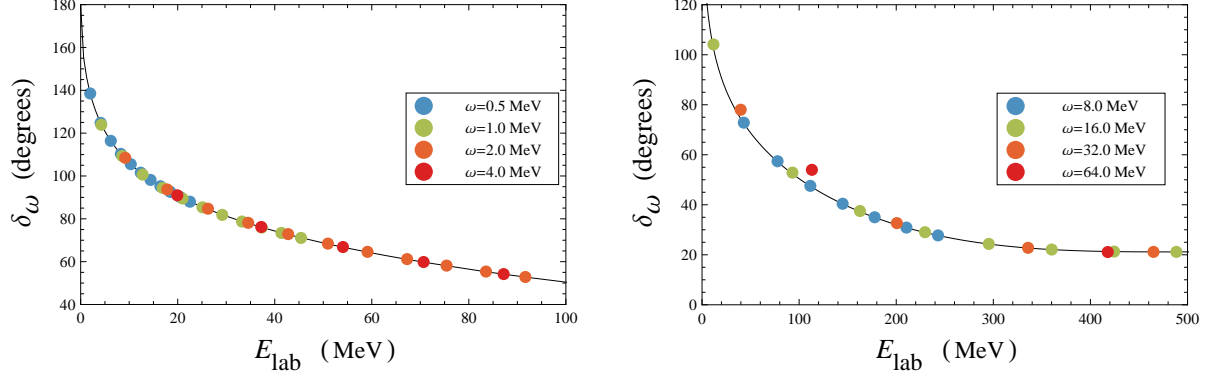


FIG. 1: (Color online) Extracted phase-shifts for the spherical-well toy-model for oscillator frequencies from  $\omega = 0.5$  MeV to  $\omega = 4.0$  MeV (left panel), and from  $\omega = 8.0$  MeV to  $\omega = 64.0$  MeV (right panel). For each oscillator frequency, the phase shift was determined from the lowest eleven energy-eigenvalues (excluding the bound state). The exact continuum phase shift, given by eq. (14), is the solid black curve. Appreciable deviations in the phase shift at larger oscillator frequencies are due to the finite range of the spherical well.

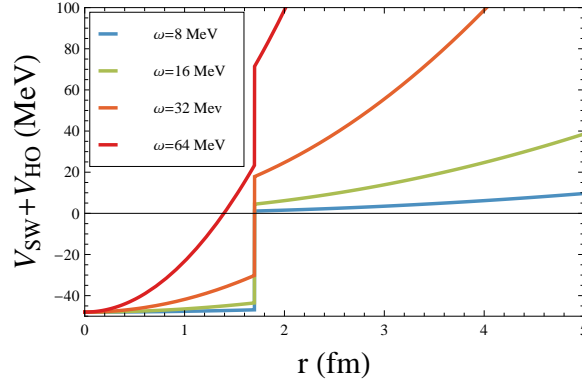


FIG. 2: (Color online) The potential between two particles interacting via a spherical well,  $V_{SW}$ , confined by a harmonic potential,  $V_{HO}$ , for different oscillator frequencies. As the oscillator frequency increases the distortion of the spherical well increases.

An interesting feature of these finite-range effects is that for a given oscillator frequency, the effects are largest at lower energy, and diminish as the energy of the system increases<sup>4</sup>.

<sup>4</sup> In the high-energy limit, in which the nucleon wavelength inside the range of the nuclear interaction is small compared to the length scale over which the potential varies significantly, the LO contribution of the harmonic potential to the s-wave phase shift, calculated in the WKB approximation, is

$$\delta_\omega(E) - \delta_{\omega=0}(E) = \frac{1}{2\sqrt{2}} \mu^{3/2} \omega^2 \int_0^\infty dx x^2 \left[ \frac{1}{\sqrt{E - V_{NN}(x)}} - \frac{1}{\sqrt{E}} \right], \quad (15)$$

where  $\mu$  is the reduced mass of the two-nucleon system, and  $V_{NN}(x)$  is the (central) NN potential. In the case of a toy model of NN interactions where a spherical well of depth  $V_0$  and radius  $R_0$  is used to describe the NN potential ( $V_0$  and  $R_0$  are tuned to reproduce the scattering length and effective range),



#### IV. REALISTIC NUCLEAR FORCES

It is important to determine how well this method works for realistic NN interactions. There are a number of modern NN potentials that could be used for this numerical comparison, but for simplicity we work with the JISP16 potential [31–33]. This  $NN$  interaction is constructed so as to reproduce the measured NN scattering phase shifts to high precision over a wide range of energies, below  $E_{\text{lab}} \lesssim 350$  MeV, and is known to provide a good description of  $p$  shell nuclei [31, 33] without an additional  $3N$  interaction. It was developed using inverse scattering techniques, followed by off-shell tuning with phase-equivalent transformations to describe selected light nuclear properties up to  $^{16}\text{O}$ . Using this interaction, the spectrum of the two confined particles was found by diagonalizing the Hamiltonian in the relative HO basis space for each partial wave. The size of the HO basis was increased until the spectrum converged to a prescribed precision. In order to access the lower energy phase shifts, we decreased  $\omega$  which consequently required an increase in the size of the basis space to obtain convergence. This limited the range of small  $\omega$  that we investigated ( $\omega \geq 0.4$  MeV with a maximum basis dimension of  $1800 \times 1800$ ). In order to improve convergence with increasing basis-space dimension, the choice of the HO frequency for the basis space was adjusted independently of the frequency of the external confining potential.

In Figs. 3 to 6 we show the application of eq. (2) to four different partial waves in the  $NN$  system:  $^1S_0$  ( $l = 0$ ),  $^3P_0$  ( $l = 1$ ),  $^3D_2$  ( $l = 2$ ) and  $^1F_3$  ( $l = 3$ ). The extracted phase-shifts were obtained from the low-lying spectrum of the  $NN$  system in harmonic potentials with a range of frequencies (the points in each figure). For comparison, the phase-shifts calculated by solving the Schrödinger equation in the absence of the harmonic potential are shown as the solid curves in each figure.

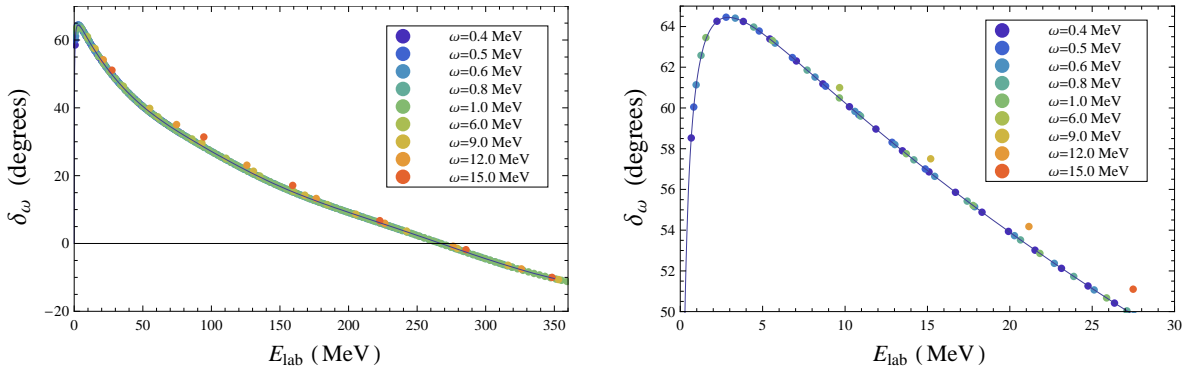


FIG. 3: (Color online) The phase-shift in the  $^1S_0$ -channel,  $\delta_\omega(E_{\text{lab}})$ , evaluated at the energy-eigenvalues determined for a range of values of  $\omega$  defining the external harmonic potential, using eq. (2). The solid curve corresponds to the phase-shift,  $\delta_{\omega=0}(E_{\text{lab}})$ , determined by a direct evaluation in free-space. The right panel is a magnification of the left panel.

the correction to the phase shift is

$$\delta_\omega(E) - \delta_{\omega=0}(E) \rightarrow \frac{1}{4\sqrt{2}} \left(\frac{\mu}{E}\right)^{3/2} \omega^2 \int_0^\infty dx x^2 V_{NN}(x) = \frac{1}{12\sqrt{2}} \left(\frac{\mu}{E}\right)^{3/2} \omega^2 V_0 R_0^3 \quad . \quad (16)$$

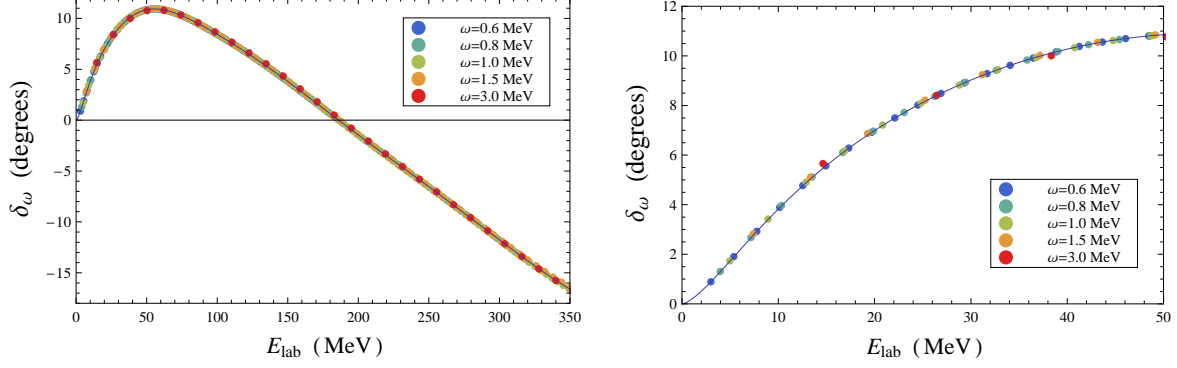


FIG. 4: (Color online) The phase-shift in the  $^3P_0$ -channel,  $\delta_\omega(E_{\text{lab}})$ , evaluated at the energy-eigenvalues determined for a range of values of  $\omega$  defining the external harmonic potential, using eq. (2). The solid curve corresponds to the phase-shift,  $\delta_{\omega=0}(E_{\text{lab}})$ , determined by a direct evaluation in free-space. The right panel is a magnification of the left panel.

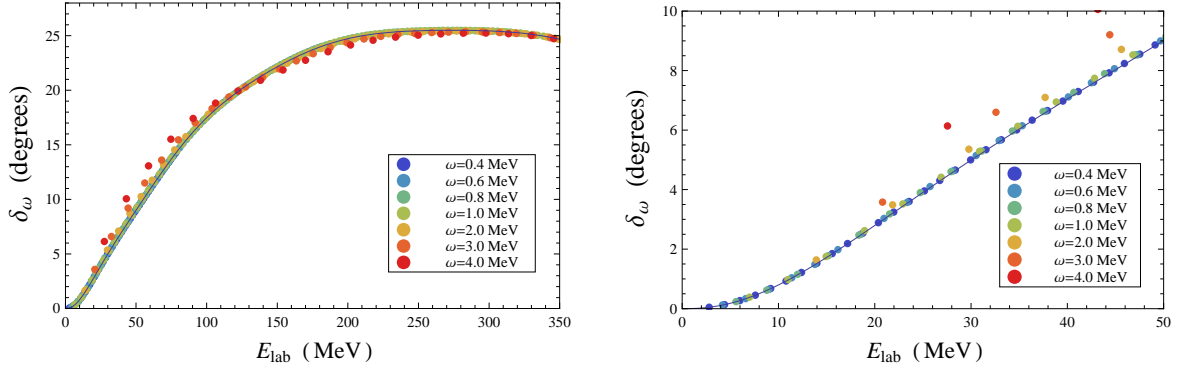


FIG. 5: (Color online) The phase-shift in the  $^3D_2$ -channel,  $\delta_\omega(E_{\text{lab}})$ , evaluated at the energy-eigenvalues determined for a range of values of  $\omega$  defining the external harmonic potential, using eq. (2). The solid curve corresponds to the phase-shift,  $\delta_{\omega=0}(E_{\text{lab}})$ , determined by a direct evaluation in free-space. The right panel is a magnification of the left panel.

### A. Numerical Analysis

The harmonic potential modifies the interactions between the two nucleons at all distance scales, and as such, there are modifications to the potential between the nucleons over the range of the nuclear forces, leading to short-distance corrections to the relation between  $p \cot \delta$  and the energy-eigenvalues given by eq. (2). The energy-eigenvalues are calculated in a given energy-interval for a range of values of  $\omega$  in order to extrapolate the phase-shift  $\delta_\omega(E_{\text{lab}})$ , to the  $\omega = 0$  limit,  $\delta_{\omega=0}(E_{\text{lab}})$ , and hence eliminate the modifications to the nuclear force due to the harmonic potential. This procedure is not as straightforward as it naively appears due to the fact that for each value of  $\omega$ , the energy-eigenvalues (generally) have different values, and an interpolation of  $\delta_\omega(E_{\text{lab}})$  within the energy-interval is required for each  $\omega$  in order to extrapolate to  $\delta_{\omega=0}(E_{\text{lab}})$  at any given energy <sup>5</sup>. For the sake of

<sup>5</sup> For a given energy, a range of values of  $\omega$  could be iteratively tuned to produce the same energy-eigenvalue.

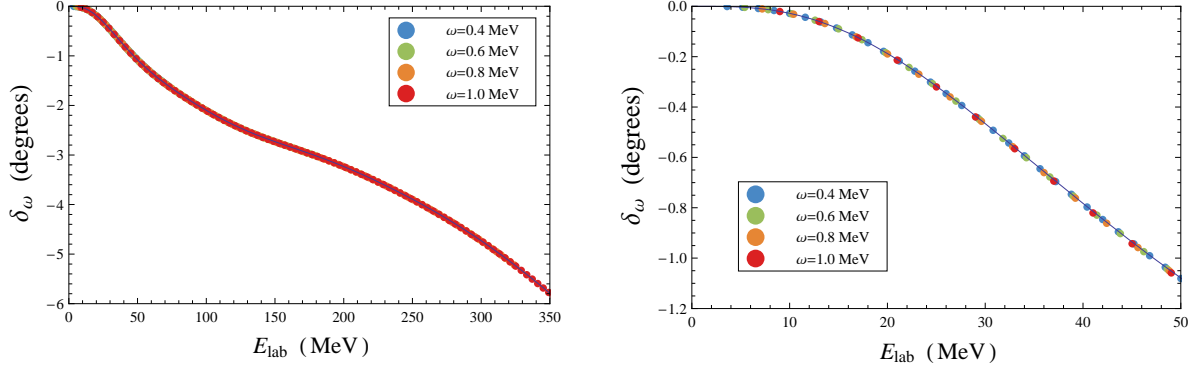


FIG. 6: (Color online) The phase-shift in the  $^1F_3$ -channel,  $\delta_\omega(E_{\text{lab}})$ , evaluated at the energy-eigenvalues determined for a range of values of  $\omega$  defining the external harmonic potential, using eq. (2). The solid curve corresponds to the phase-shift,  $\delta_{\omega=0}(E_{\text{lab}})$ , determined by a direct evaluation in free-space. In the left panel this solid curve is obscured by the points calculated using eq. (2). The right panel is a magnification of the left panel.

demonstration, we focus on the phase-shift in the  $^1S_0$  channel, but the methodology can be applied in all channels.

The energy-eigenvalues of two nucleons interacting in the  $^1S_0$  in a harmonic potential were calculated for a range of values of  $\omega$  from  $\omega = 0.4$  MeV to  $\omega = 15.0$  MeV. For each eigenvalue, the scattering phase-shift  $\delta_\omega(E_{\text{lab}})$  was calculated using the zero-range relation in eq. (2), the results of which are shown in Fig. 3. The “exact” phase-shift  $\delta_{\omega=0}(E_{\text{lab}})$  that is determined by solving the Schrödinger equation for the phase-shift in the absence of the external harmonic potential is shown in Fig. 3 as the solid curve. For  $\omega \lesssim 1.0$  MeV, and for the energy-eigenvalues shown in Table I, the phase-shift calculated from the zero-range relation in eq. (2) is very close to the actual phase-shift. For larger values of  $\omega$  there are noticeable deviations from the exact result, but these deviations are found to become smaller as the energy increases.

The energy-dependent interpolation of the phase-shift for a given  $\omega$  that is required in order to extrapolate  $\delta_\omega(E_{\text{lab}})$  to  $\delta_{\omega=0}(E_{\text{lab}})$  is the most problematic part of this numerical analysis. In the range of energies for which the ERE is formally convergent ( $|\mathbf{p}| \leq m_\pi/2$  resulting from the location of the t-channel cut in the one-pion exchange amplitude) an expansion of  $p \cot \delta$  in powers of the energy reproduces the scattering amplitude. In contrast, for energies outside of this range, but below the inelastic threshold (for which the relation between  $p \cot \delta$  and the energy-eigenvalues in the harmonic potential in eq. (2) remains valid) such a power-series does not describe the amplitude. As such, without directly solving for the amplitude, one does not know the form to use for the interpolation in relative energy  $E$  beyond  $|\mathbf{p}| = m_\pi/2$ . We do not attempt to resolve this issue, and restrict ourselves to the energy range for which the ERE formally converges<sup>6</sup>. In Fig. 7 we show the extracted values of  $p \cot \delta$  as a function of relative energy  $E$  for  $\omega \leq 1$  MeV. For each  $\omega \leq 1$  MeV a fourth-order polynomial in  $E$  is fit to the values of  $p \cot \delta$  shown in Fig. 7 (the order was chosen to minimize the  $\chi^2/\text{dof}$  of the fit and to achieve a stable fit under the change of

<sup>6</sup> Within this range, this part of our analysis is formally equivalent to the pionless EFT description given in Refs. [19, 34].

TABLE I: The lowest eight energy-eigenvalues in the center-of-mass frame and their associated phase-shifts found from eq.(2) in the  $^1S_0$ -channel for  $\omega \leq 1$  MeV.

	$\omega = 0.4$ MeV	$\omega = 0.5$ MeV	$\omega = 0.6$ MeV	$\omega = 0.8$ MeV	$\omega = 0.9$ MeV	$\omega = 1.0$ MeV
$E_1$	0.66642	0.81618	0.96488	1.2610	1.40898	1.55711
$\delta_\omega(E_1)$	58.5279	60.0449	61.1382	62.5816	63.0684	63.4511
$E_2$	2.22732	2.78198	3.33893	4.4597	5.02344	5.58933
$\delta_\omega(E_2)$	64.2586	64.45411	64.4124	63.9721	63.6576	63.3088
$E_3$	3.82836	4.7907	5.75672	7.69914	8.67518	9.65424
$\delta_\omega(E_3)$	64.2495	63.7768	63.1847	61.8606	61.1775	60.4948
$E_4$	5.4363	6.80548	8.17932	10.9398	12.326	13.7158
$\delta_\omega(E_4)$	63.3856	62.4755	61.5194	59.6034	58.6685	57.754
$E_5$	7.04598	8.82126	10.602	14.1783	15.9733	17.7726
$\delta_\omega(E_5)$	62.3082	61.0673	59.832	57.4512	56.3152	55.214
$E_6$	8.65604	10.8369	13.0238	17.4144	19.6173	21.825
$\delta_\omega(E_6)$	61.1822	59.6694	58.2013	55.4272	54.1198	52.8615
$E_7$	10.266	12.852	15.4446	20.6482	23.2584	25.8736
$\delta_\omega(E_7)$	60.0611	58.3139	56.6418	53.5231	52.0696	50.6769
$E_8$	11.8758	14.8665	17.8645	23.8802	26.897	29.9188
$\delta_\omega(E_8)$	58.9638	57.0076	55.1527	51.7288	50.1421	48.6454

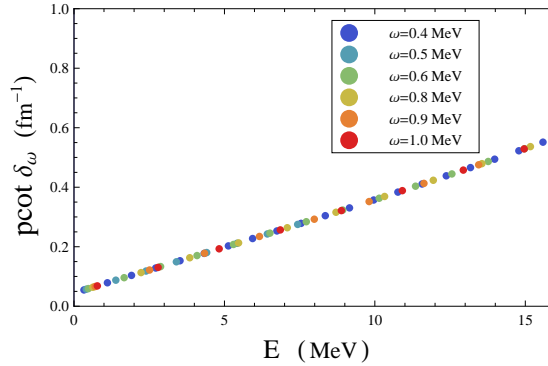


FIG. 7: (Color online)  $p \cot \delta$  as a function of the energy in the center-of-mass frame in the  $^1S_0$ -channel extracted from the energy-eigenvalues of the two-nucleon system in harmonic potentials for a range of oscillator frequencies  $\omega$ .

order <sup>7</sup>). With the interpolating functions, it is then possible to choose a particular value of  $E$  and extrapolate  $p \cot \delta_\omega(E)$  to  $p \cot \delta_{\omega=0}(E)$ , from which the phase-shift  $\delta_{\omega=0}(E)$  can be recovered. The  $\omega$ -extrapolations at  $E = 1$  MeV and  $E = 5$  MeV are shown in Fig. 8. A fit function of the form  $p \cot \delta_\omega = A + B \omega^2$  is used to extrapolate to  $\omega = 0$ , as also shown in Fig. 8. The small observed scatter of the points about the best fit function is attributed to the form of the interpolation in  $E$  (and the increasing separation between energy-eigenvalues

<sup>7</sup> A full systematic study of uncertainties would include the variation of the fit with the polynomial order.

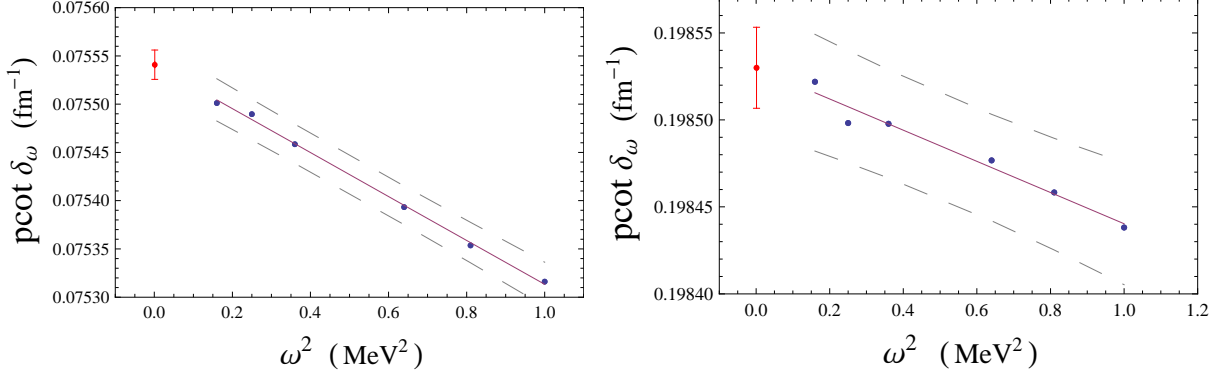


FIG. 8: (Color online) The extrapolation of  $p \cot \delta_\omega(E)$  to  $p \cot \delta_{\omega=0}(E)$  in the  $^1S_0$ -channel at  $E = 1$  MeV (left panel) and  $E = 5$  MeV (right panel). The solid lines correspond to the best fits of the form  $p \cot \delta_\omega = A + B \omega^2$ , and the dashed lines correspond to the 99% confidence intervals. The red points with their associated 1-sigma uncertainties correspond to  $\delta_{\omega=0}(E)$ .

with increasing  $\omega$ ), and not the finite model-space as the energy-eigenvalues have converged to six significant digits which we establish by increasing  $N_{MS}$  sufficiently. An important point to note is that the results of the calculations at the smallest few values of  $\omega$  are all within  $\sim 0.1\%$  of the extrapolated values. Therefore, to determine the phase-shift at this level of precision, no extrapolation in  $\omega^2$  is required. The extrapolated phase-shift  $\delta_{\omega=0}(E_{\text{lab}})$  in the  $^1S_0$ -channel is shown in Fig. 9, and is found to agree with the exact phase-shift (the solid curve) within the uncertainties of the calculation. The points with uncertainties correspond to the phase-shift derived from the energy-eigenvalues extrapolated to  $\omega = 0$  evaluated at regular intervals in  $E$ . Uncertainties in the extrapolated phase-shifts, which are at the  $\sim 10^{-4}$ -level, can, in principle, be reduced further by calculating at even smaller values of  $\omega$ .

We have numerically explored some of the higher partial-waves. The methodology in the higher partial-waves is the same as in the  $^1S_0$ -channel. The harmonic potential modifications to the nuclear force are seen to increase with increasing partial-wave. This behavior is expected due to the fact that the centripetal barrier, and the associated  $r^l$  behavior of the wavefunction near the origin, forces the wavefunction to larger values of  $r$  (but within the range of the nuclear force) and hence to larger values of the harmonic potential. Calculations at smaller values of  $\omega$  than employed for the S-wave case are required in order to achieve the same level of precision, consistent with the conclusions of Ref. [37]. The extracted values of the phase-shift in the  $^3P_0$ ,  $^3D_2$  and  $^1F_3$  channels extrapolated to  $\omega = 0$  are shown in Fig. 10. In all channels, the extrapolated phase-shifts are found to agree with the “exact” phase-shift within the uncertainties of the calculation.

Determining the energy levels of two nucleons in a harmonic potential involves calculating the matrix elements of the full Hamiltonian, including the harmonic potential, in a large model-space, with a cutoff on relative excitation energies denoted by  $\omega N_{MS}$ . In the limit that  $N_{MS} \rightarrow \infty$  the energy-eigenvalues found by diagonalizing the  $N_{MS} \times N_{MS}$  Hamiltonian will coincide with the exact energy-eigenvalues. For a finite-dimensional space, the energy-eigenvalues deviate from their infinite model-space values as shown, for instance, in Fig. 11, making the quantification of the convergence of eigenvalues with respect to  $N_{MS}$  highly non-trivial. We do not attempt to resolve this issue here, and all of the energy-eigenvalues we

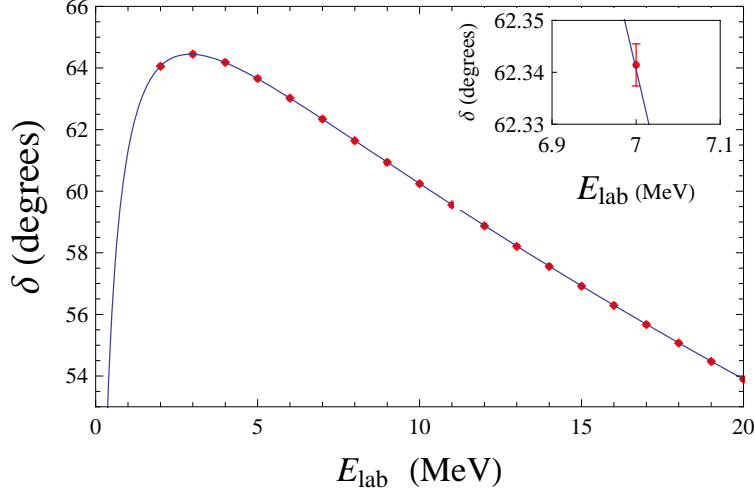


FIG. 9: (Color online) The  $\omega$ -extrapolated phase-shift  $\delta_{\omega=0}(E_{\text{lab}})$  as a function of  $E_{\text{lab}}$  in the  $^1S_0$ -channel. The points and their uncertainty are determined, at uniform intervals in  $E_{\text{lab}}$ , by the interpolations and extrapolations described in the text. The solid curve corresponds to the “exact” phase-shift. The inset is a magnification around  $E_{\text{lab}} = 7$  MeV that shows the precision of the calculation.

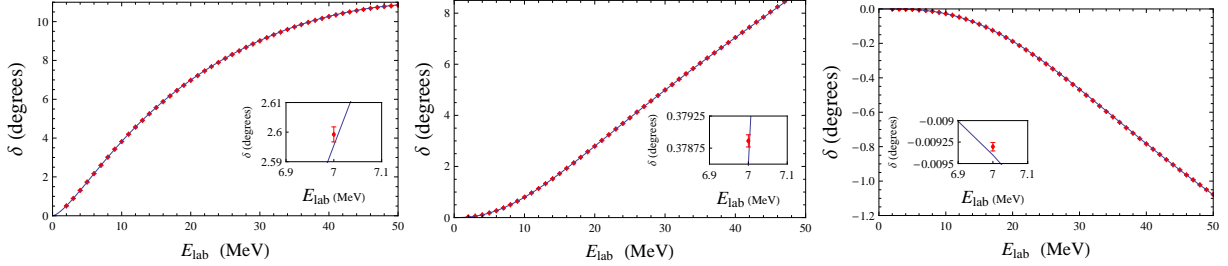


FIG. 10: (Color online) The  $\omega$ -extrapolated phase-shift  $\delta_{\omega=0}(E_{\text{lab}})$  as a function of  $E_{\text{lab}}$  in the  $^3P_0$ -channel (left panel), the  $^3D_2$ -channel (center panel) and the  $^1F_3$ -channel (right panel). The insets are a magnification around  $E_{\text{lab}} = 7$  MeV that shows the precision of the calculations.

have used in this work have converged to at least six significant digits.

In this work we have only analyzed uncoupled channels for simplicity. In general, due to the spin of the nucleon, and the fact that two nucleons can have  $S = 1$ , many two-nucleon states with total angular momentum  $J$  are a linear combination of two orbital

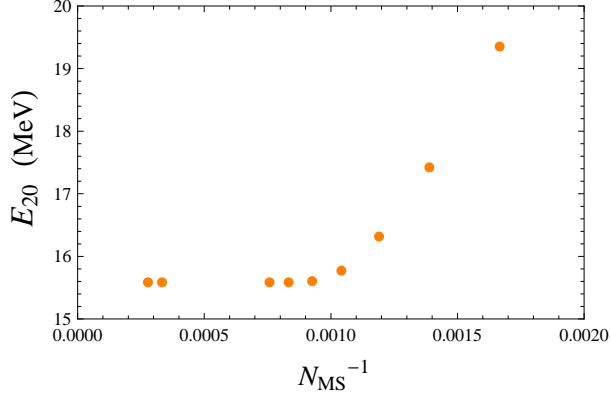


FIG. 11: (Color online) The 20<sup>th</sup> energy-eigenvalue in the center-of-mass frame for the  $^1S_0$ -channel with  $\omega = 0.4$  MeV as a function of the inverse cut-off of the model-space,  $1/N_{\text{MS}}$ .

angular momentum states, such as the  $^3S_1$ - $^3D_1$  coupled-channel which contains the deuteron. The zero-range relation between the energy-eigenvalues in the harmonic potential and the scattering phase shift, given in eq. (2), will be modified to be a relation involving the three scattering parameters that describe a two-component coupled-channels system, e.g.  $\delta_0$ ,  $\delta_2$  and  $\epsilon_1$ , and not just a simple relation between one phase shift and the energy-eigenvalues. Such relations remain to be constructed for two nucleons in a harmonic potential. As the  $^3S_1$ - $^3D_1$  coupled-channels system contains the deuteron as a bound-state, we can explore the behavior of the lowest energy-eigenvalue as a function of  $\omega$ . The perturbative corrections to the location of such bound states due to the presence of the harmonic potential are given in eq. (4), where the LO deviations scale as  $\sim \omega^2$ . The binding energies are found to be  $E_0 = -2.2209$  MeV,  $-2.2163$  MeV,  $-2.2098$  MeV, and  $-2.2017$  MeV in harmonic potentials with  $\omega = 0.2$  MeV,  $0.3$  MeV,  $0.4$  MeV and  $0.5$  MeV, respectively. The extrapolation of these values to  $\omega = 0$  is shown in Fig. 12. The results are fit well by a polynomial of the form  $E_0 = E_0^{(\omega=0)} + C \omega^2 + D \omega^4 + F \omega^6$ , where  $C, D, F$  and  $E_0^{(\omega=0)}$  are fit variables, for the range of  $\omega$  for which the calculations have been performed. The deuteron binding energy extracted from the extrapolation to  $\omega = 0$  is  $E_0^{(\omega=0)} = -2.22466(4)$  MeV (which is to be compared with the input value of  $-B_0 = -2.224575$  MeV). The coefficient of the  $\omega^2$  term is  $C_{\text{fit}} = 0.0939(4)$ , which is consistent with the value expected in the zero-range limit of  $C_{\text{ZR}} = 0.0944$  from eq. (6). One expects both the LO short-range contributions from  $\omega \neq 0$  and the small D-state admixture due to the tensor force to also depend upon  $\omega^2$ , and to modify the value of  $C$  away from  $C_{\text{ZR}}$ , but it is clear from this work that such deviations are small.

By looking at different energy eigenvalues, the effective range parameters can be extracted through the relation

$$p^{2l+1} \cot \delta_l(p) = -1/a_l + 1/2 r_l p^2 + \dots = -1/a_l + 1/2 r_l m E + \dots, \quad (17)$$

where  $E$  is any relative energy eigenvalue which is low enough to ensure convergence of the ERE. For example, the low-energy spectrum of the confined  $^1S_0$  system can be used to extract the scattering length and effective range using eq. (2). We show these extracted parameters at the  $1\text{-}\sigma$  level in Fig. (13). These extracted parameters vary with  $\omega^2$  in a way that is consistent with expectations and converge to the exact result. For a system with ERE parameters that are of natural size, the perturbative expressions from sect. II B

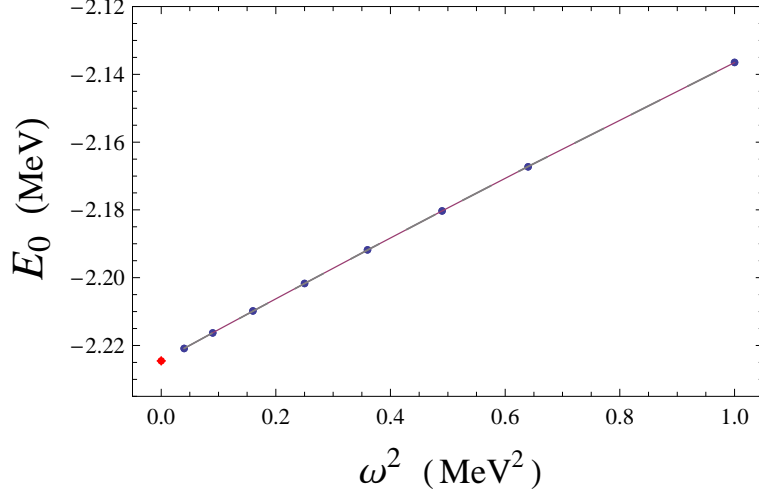


FIG. 12: (Color online) The deuteron binding energy as a function of  $\omega^2$ . The solid line corresponds to the best fit of the form  $E_0 = E_0^{(\omega=0)} + C \omega^2 + D \omega^4 + F \omega^6$ , and the dashed lines (practically indistinguishable from the solid line) denote the 68% confidence interval. The red point corresponds to the ground state energy obtained by extrapolating to  $\omega = 0$ . The uncertainty is within the size of the red point.

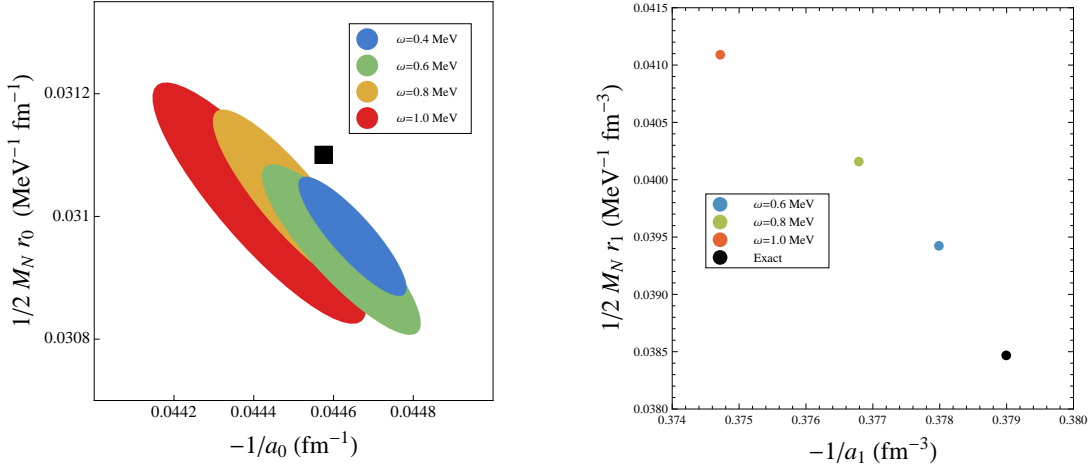


FIG. 13: (Color online) The extracted  $^1S_0$  (left panel) and  $^3P_0$  (right panel) scattering lengths and effective ranges for different harmonic potentials. The exact values are denoted by the black points. The ellipses on the left panel denote the 68% confidence intervals and were determined by fitting the ERE to the interpolated phase-shift at a given value of  $\omega$ . The parameters in the right panel were determined by fitting the three lowest states of the spectrum to the perturbative expressions of sect. II B.

can also be used to extract these parameters. In Fig. 13 the extracted ‘scattering volume’,  $a_1$ , and ‘effective momentum’,  $r_1$ , in the  $^3P_0$  channel, determined through the perturbative expressions, are shown. The behavior as  $\omega^2 \rightarrow 0$  is consistent with the exact result.



## V. CONCLUSION

The NN phase-shift below the inelastic threshold can be determined from the eigenvalue spectrum of two interacting nucleons confined to move in a harmonic oscillator potential. The conventional discussions of scattering from a potential that falls faster than  $1/r$ , and the connection between the scattering amplitude and the location of poles in the complex energy-plane corresponding to bound-states is complicated by the fact that the harmonic potential is confining and asymptotic scattering states cannot be defined for any non-zero value of the harmonic oscillator frequency,  $\omega$ . As a result, the zero-range relation between the scattering phase-shift and the energy-eigenvalues is modified by the non-zero value of the harmonic potential within the range of the nuclear interaction, giving rise to finite-range corrections. These corrections are not present when dealing with a pionless EFT description of two nucleons confined within a harmonic trap (when the cutoff is taken to infinity). However, any pionful theory of the nuclear interaction that describes nuclear processes above the t-channel cut will have to address these finite-range issues.

We have studied these aspects numerically for two nucleons confined by a harmonic potential. The nuclear interaction was modeled by the JISP16 potential, but our results are general and can be applied to other phenomenological or chiral effective field theory interactions. We have explored uncoupled channels and found that for small values of  $\omega$ , the low-energy phase shift can be extracted from the energy-eigenvalues through an extrapolation to  $\omega = 0$ . At the level of precision to which we have performed the calculations, the energy-eigenvalues combined with the zero-range relation supplemented by an extrapolation to  $\omega = 0$  allow for the determination of the low-energy NN elastic scattering phase shifts. Further, such calculations enable a precise determination of the deuteron binding energy.

Since the methods we present here are clearly non-perturbative and include all antisymmetrization effects, an interesting application of eq. (2) would be to the elastic scattering of two nuclear systems, with one or both composed of more than one nucleon, below inelastic and re-arrangement thresholds [18]. The processes we have in mind are  $nd$ ,  $nt$  and  $n\alpha$  scattering. Calculations of three-, four-, and five-nucleon systems can be performed within harmonic potentials with small  $\omega$  (to access low-energy phase shifts and minimize finite-range effects), and an application of eq. (2), modified by the reduced mass and an appropriate subtraction for the center-of-mass energy, and extrapolation to  $\omega = 0$  would give the scattering phase-shift at low energies. This method contrasts with those currently in use, such as Faddeev [39], Faddeev-Yakubovsky [40], AGS [41], Hyperspherical Harmonics [42, 43], NCSM/RGM [44], GFMC [45], and J-matrix methods [46]. There remains technical challenges to obtaining sufficient convergence with increasing  $N_{MS}$  and/or to extending the corrections for finite  $\omega$  to higher order terms. A possible strategy to alleviate such issues is through the use of HO-based EFT methods [13, 20]. Work in this direction is under way.

## Acknowledgments

TL and MJS thank the co-organizers of the INT workshop “Simulations and Symmetries: Cold Atoms, LQCD, and Few-Hadron Systems”, H. Hammer and D. Phillips, for providing a stimulating environment in which part of this work was accomplished. We thank S. Beane, A. Nicholson, S. Quaglioni, and I. Stetcu for their critical reading of this manuscript. We also thank A. I. Mazur and A. M. Shirokov for providing valuable scattering phase shifts

for the JISP16 interaction from solving the Schrödinger equation. The work of TL was performed under the auspices of the U.S. Department of Energy by Lawrence Livermore National Laboratory under Contract DE-AC52-07NA27344 and the UNEDF SciDAC grant DE-FC02-07ER41457. The work of MJS was supported in part by the U.S. Dept. of Energy under Grant No. DE-FG03-97ER4014. The work of JPV was supported in part by the U.S. Dept. of Energy under Grant No. DE-FG02-87ER40371. The work of AS was supported in part by the Natural Sciences and Engineering Research Council of Canada (NSERC) and the Helmholtz Alliance Program of the Helmholtz Association, contract HA216/EMMI “Extremes of Density and Temperature: Cosmic Matter in the Laboratory”. TRIUMF receives funding via a contribution through the National Research Council Canada.

- 
- [1] P. Navratil, J. P. Vary and B. R. Barrett, Phys. Rev. Lett. **84**, 5728 (2000), Phys. Rev. C **62**, 054311 (2000).
  - [2] P. Navratil, V. G. Gueorguiev, J. P. Vary, W. E. Ormand and A. Nogga, Phys. Rev. Lett. **99**, 042501 (2007) [arXiv:nucl-th/0701038].
  - [3] S. C. Pieper, Riv. Nuovo Cim. **031**, 709 (2008) [arXiv:0711.1500 [nucl-th]].
  - [4] S. C. Pieper, R. B. Wiringa and J. Carlson, Phys. Rev. C **70**, 054325 (2004) [arXiv:nucl-th/0409012].
  - [5] G. Hagen, T. Papenbrock, D. J. Dean and M. Hjorth-Jensen, Phys. Rev. Lett. **101**, 092502 (2008) [arXiv:0806.3478 [nucl-th]].
  - [6] G. Hagen, T. Papenbrock, D. J. Dean, A. Schwenk, A. Nogga, M. Wloch and P. Piecuch, Phys. Rev. C **76**, 034302 (2007) [arXiv:0704.2854 [nucl-th]].
  - [7] A. M. Lane and R. G. Thomas, Rev. Mod. Phys. **30**, 257 (1958)
  - [8] P. Descouvemont and D. Baye, Rept. Prog. Phys. **73**, 036301 (2010) [arXiv:1001.0678 [nucl-th]].
  - [9] K. Langanke, Nucl. Phys. A **457**, 351 (1986).
  - [10] K. Fujimura, D. Baye, P. Descouvemont, Y. Suzuki and K. Varga, Phys. Rev. C **59**, 817 (1999).
  - [11] B. Pfitzinger, H. M. Hofmann and G. M. Hale, Phys. Rev. C **64**, 044003 (2001) [arXiv:nucl-th/0010091].
  - [12] S. Quaglioni and P. Navratil, Phys. Rev. Lett. **101**, 092501 (2008) [arXiv:0804.1560 [nucl-th]].
  - [13] W. C. Haxton, arXiv:0710.0289 [nucl-th].
  - [14] W. C. Haxton and T. Luu, Phys. Rev. Lett. **89**, 182503 (2002) [arXiv:nucl-th/0204072].
  - [15] I. Stetcu, B. R. Barrett and U. van Kolck, Phys. Lett. B **653**, 358 (2007) [arXiv:nucl-th/0609023].
  - [16] T. Luu and A. Schwenk, Phys. Rev. Lett. **98**, 103202 (2007) [arXiv:cond-mat/0606069].
  - [17] I. Stetcu, B. R. Barrett, U. van Kolck and J. P. Vary, Phys. Rev. A **76**, 063613 (2007) [arXiv:0705.4335 [cond-mat.other]].
  - [18] I. Stetcu, J. Rotureau, B. R. Barrett and U. van Kolck, J. Phys. G **37**, 064033 (2010) [arXiv:0912.3015 [nucl-th]].
  - [19] U. van Kolck, “Nuclear Physics from QCD”, talk given at DOE workshop *Forefront Questions in Nuclear Science and the Role of High Performance Computing*, Jan. 2009. <http://extremecomputing.labworks.org/nuclearphysics/index.stm>
  - [20] I. Stetcu, J. Rotureau, B. R. Barrett and U. van Kolck, arXiv:1001.5071 [cond-mat.quant-gas].

- [21] J.-W. Lee, A. N. Nicholson, M. Endres and D. B. Kaplan, “Trapped Unitary Fermions,” talk given at INT workshop *LQCD, Cold Atoms, and Few-Hadron Systems*, [www.int.washington.edu/talks/WorkShops/int\\_10\\_1/](http://www.int.washington.edu/talks/WorkShops/int_10_1/)
- [22] H. W. Hamber, E. Marinari, G. Parisi and C. Rebbi, Nucl. Phys. B **225**, 475 (1983).
- [23] M. Lüscher, Commun. Math. Phys. **105**, 153 (1986).
- [24] M. Lüscher, Nucl. Phys. B **354**, 531 (1991).
- [25] M. A. Preston and I. Bhadhuri, Structure of the Nucleus, published by Westview Press (1973); ISBN 0-201-62729-9.
- [26] E. Epelbaum, H. Krebs, D. Lee and U. G. Meissner, arXiv:1003.5697 [nucl-th].
- [27] L. Maiani and M. Testa, Phys. Lett. B **245** (1990) 585.
- [28] S. R. Beane, W. Detmold, K. Orginos and M. J. Savage, arXiv:1004.2935 [hep-lat].
- [29] P. F. Bedaque, I. Sato and A. Walker-Loud, Phys. Rev. D **73**, 074501 (2006) [arXiv:hep-lat/0601033].
- [30] S. R. Beane, P. F. Bedaque, A. Parreno and M. J. Savage, Phys. Lett. B **585**, 106 (2004) [arXiv:hep-lat/0312004].
- [31] A. M. Shirokov, J. P. Vary, A. I. Mazur, and T. A. Weber, Phys. Lett. B **644**, 33 (2007).
- [32] A Fortran code for the JISP16 interaction matrix elements is available at <http://nuclear.physics.iastate.edu>.
- [33] P. Maris, J. P. Vary, and A. M. Shirokov, Phys. Rev. C **79**, 014308 (2009).
- [34] I. Stetcu, “Cold Atoms in Traps”, talk given at INT workshop *Simulations and Symmetries: Cold Atoms, LQCD, and Few-Hadron Systems*, Apr. 2010. [www.int.washington.edu/PROGRAMS/10-1.html](http://www.int.washington.edu/PROGRAMS/10-1.html)
- [35] T. Busch, B.-G. Englert, K. Rzazewski and M. Wilkens, Foundations of Physics **28**, 549 (1998).
- [36] S. K. Yip, Phys. Rev. A **78**, 013612 (2008).
- [37] A. Suzuki, Y. Liang and R. K. Bhaduri, Phys. Rev. A **80**, 033601 (2009).
- [38] T. Mehen, arXiv:0712.0867 [cond-mat.other].
- [39] H. Witala, J. Golak, W. Glockle and H. Kamada, Phys. Rev. C **71**, 054001 (2005) [arXiv:nucl-th/0412063].
- [40] R. Lazauskas, J. Carbonell, A. C. Fonseca, M. Viviani, A. Kievsky and S. Rosati, Phys. Rev. C **71**, 034004 (2005) [arXiv:nucl-th/0412089].
- [41] A. Deltuva and A. C. Fonseca, Phys. Rev. C **79**, 014606 (2009) [arXiv:0901.0875 [nucl-th]].
- [42] L. E. Marcucci, L. Girlanda, A. Kievsky, S. Rosati and M. Viviani, J. Phys. Conf. Ser. **168**, 012005 (2009).
- [43] M. Viviani, A. Kievsky, L. Girlanda and L. E. Marcucci, Few Body Syst. **45**, 119 (2009) [arXiv:0812.3547 [nucl-th]].
- [44] S. Quaglioni and P. Navratil, Phys. Rev. C **79**, 044606 (2009) [arXiv:0901.0950 [nucl-th]].
- [45] K. M. Nollett, S. C. Pieper, R. B. Wiringa, J. Carlson and G. M. Hale, Phys. Rev. Lett. **99**, 022502 (2007) [arXiv:nucl-th/0612035].
- [46] A. M. Shirokov, A. I. Mazur, J. P. Vary and E. A. Mazur, Phys. Rev. C **79**, 014610 (2009) [arXiv:0806.4018 [nucl-th]].